Intraoperative evaluation of revascularization effect on ischemic muscle hemodynamics using near-infrared diffuse optical spectroscopies

Guoqiang Yu,[a] Yu Shang,[a] Youquan Zhao,[a,b] Ran Cheng,[a] Lixin Dong,[a] and Sibu P. Saha[c]
[a]University of Kentucky, Center for Biomedical Engineering, Lexington, Kentucky 40506–0070
[b]Tianjin University, Department of Biomedical Engineering, Tianjin 300072, China
[c]University of Kentucky, Cardiothoracic Surgery, Lexington, Kentucky 40536–0200

Abstract. Arterial revascularization in patients with peripheral arterial disease (PAD) reestablishes large arterial blood supply to the ischemic muscles in lower extremities via bypass grafts or percutaneous transluminal angioplasty (PTA). Currently no gold standard is available for assessment of revascularization effects in lower extremity muscles. This study tests a novel near-infrared diffuse correlation spectroscopy flow-oximeter for monitoring of blood flow and oxygenation changes in medial gastrocnemius (calf) muscles during arterial revascularization. Twelve limbs with PAD undergoing revascularization were measured using a sterilized fiber-optic probe taped on top of the calf muscle. The optical measurement demonstrated sensitivity to dynamic physiological events, such as arterial clamping/releasing during bypass graft and balloon inflation/deflation during PTA. Significant elevations in calf muscle blood flow were observed after revascularization in patients with bypass graft ($+48.1 \pm 17.5\%$) and patients with PTA ($+43.2 \pm 11.0\%$), whereas acute post-revascularization effects in muscle oxygenation were not evident. The decoupling of flow and oxygenation after revascularization emphasizes the need for simultaneous measurement of both parameters. The acute elevations/improvements in calf muscle blood flow were associated with significant improvements in symptoms and functions. In total, the investigation corroborates potential of the optical methods for objectively assessing the success of arterial revascularization. © *2011 Society of Photo-Optical Instrumentation Engineers (SPIE).* [DOI: 10.1117/1.3533320]

Keywords: diffusion; correlation; spectroscopy; muscle; blood flow; oxygenation; peripheral arterial disease; arterial revascularization.

Paper 10473R received Aug. 25, 2010; revised manuscript received Nov. 22, 2010; accepted for publication Dec. 7, 2010; published online Feb. 15, 2011.

1 Introduction

1.1 Peripheral Arterial Disease and Revascularization

Peripheral arterial disease (PAD) is a form of lower extremity atherosclerosis estimated to affect 8–12 million Americans.[1] Patients with compromised blood flow to the lower extremity may present with limb muscle ischemia, causing intermittent claudication (IC), rest pain of leg muscles, and limb loss.[2] Muscle ischemia results from an imbalance between oxygen supply (blood flow) and oxygen demand (consumption) in the affected lower extremity.

Arterial revascularization via bypass grafts or percutaneous transluminal angioplasty (PTA) is a surgical procedure for the provision of a new, additional, or augmented blood supply to a body part (e.g., lower extremity) or organ.[3] Arterial revascularization can decrease symptom severity and potentially prevent limb amputation.[4] However, reestablishing large arterial blood supply to ischemic tissues may not completely correct the underlying microvascular and/or metabolic dysfunction in muscle tissues.[5,6] An approach to assess tissue hemodynamics and metabolism in the ischemic muscle of a lower extremity could enable evaluation of revascularization success and potentially elucidate the pathophysiology contributing to the incomplete functional benefit.

1.2 Techniques for Clinical Evaluation of Revascularization

The x ray peripheral vascular angiography has been used for intraoperative verification of bypass graft patency.[7] Limitations of this technique include inability to measure flow dynamics, violation of graft integrity, risks of ionizing hazard, contrast injection, and arterial puncture.[7,8] Doppler ultrasound[7] is another clinical tool used for functional assessment of blood flow in large vessels, but has difficulty in probing small vessels [e.g., diameter less than 100 μm (Ref. 9)] in the lower extremity muscles.

Current noninvasive techniques for the evaluation of microvascular blood flow include Doppler optical coherence tomography[10] and laser Doppler.[11] Transcutaneous oximetry (TcpO$_2$) can measure local oxygen tension at the tissue surface.[12,13] However, these techniques only evaluate blood flow at the skin level, which may differ from that of deep muscles.[14]

The clinical success of revascularization is often defined by functional/symptomatic improvements such as increase of resting ankle/brachial blood pressure index (ABI) by ≥ 0.10, improvement of claudication, relief of resting pain, and healing of ulceration.[4,15] Diagnostic techniques to directly quantify tissue hemodynamic and metabolic responses to the revascularization in local ischemic muscles of a lower extremity would describe a critical feature of treatment success and lead to a better understanding of the treatment mechanisms.

Address all correspondence to: Guoqiang Yu, University of Kentucky, Center for Biomedical Engineering, Lexington, KY 40506–0070. Tel: 859–257-9110; Fax: 859–257-1856; E-mail: guoqiang.yu@uky.edu
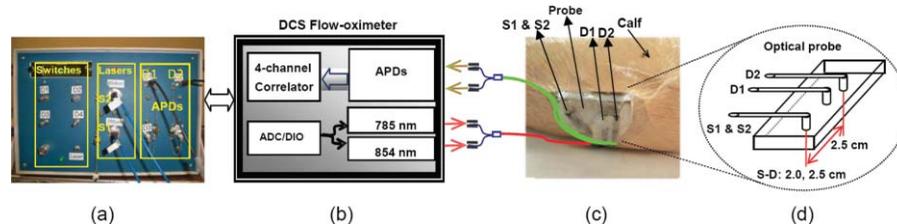
Fig. 1 DCS flow-oximeter for simultaneous measurement of muscle blood flow and oxygenation. (a) A photograph of four-channel DCS flow-oximeter (dimensions: 8″ × 12″ × 18″). (b) A diagram of four-channel DCS flow-oximeter. (c) A photograph of the fiber-optic probe taped on the surface of medial gastrocnemius (calf) muscle. (d) A fiber-optic probe with two source (S1 and S2) and two detector (D1 and D2) fibers confined to a soft-foam pad. The fiber tips were mechanically bent to turn the light 90 deg (Fiberoptics Inc., CA, USA). The tips of two source fibers (S1 and S2) were tightly bundled and placed at the same location. The distances between the source and detector fibers were 2.0 and 2.5 cm, respectively.

1.3 Near-infrared Spectroscopy (NIRS) for Measurement of Tissue Hemodynamics

A well known spectral window exists in the near-infrared (NIR) range (650–950 nm) wherein tissue absorption is relatively low so that light can penetrate into deep/thick volumes of tissues (up to several centimeters). NIRS primarily measures the tissue absorption and scattering, as well as the derived values of hemoglobin concentration and blood oxygen saturation in deep tissues.[16–20] Unlike Doppler ultrasound, NIRS is sensitive to small vessels such as arterioles, capillaries, and venules. Using NIRS, researchers have found that muscle oxygenation responses to exercise were associated with the severity of muscle vascular diseases.[19,21–27] NIRS was also used to monitor gluteal tissue oxygenation index during bypass of bilateral hypogastric artery (HA)[3] and assess bypass graft patency in large vessels.[8,28]

Skeletal muscle blood flow can be indirectly estimated by NIRS through applying venous occlusion to a limb at several discrete time-points.[25] Unfortunately, the occlusion interrupts blood flow and makes it difficult for continuous measurement of blood flow during revascularization. A novel technology, the NIR diffuse correlation spectroscopy (DCS) flowmeter, was recently developed for noninvasive and direct measurement of relative change of blood flow (rBF) in deep tissues,[29–40] including skeletal muscles.[14,41–46] The DCS flowmeter uses near-infrared (NIR) light to directly detect the motion of red blood cells in microvasculature. Unlike venous occlusion NIRS, DCS does not interrupt blood flow during measurement, and is easy to continuously perform. Very recently we extended the DCS flowmeter to measure both blood flow and oxygenation (namely DCS flow-oximeter) in human skeletal muscles.[43] The unique portable design of DCS flow-oximeter (dimensions: 8″×12″×18″) makes it possible to be used at the bedside in operating rooms.

DCS measurements of blood flow variation in various organs and tissues have been compared and validated to other standards, including power Doppler ultrasound in murine tumors,[47] laser Doppler in rat brain,[48] Xenon-CT in traumatic brain,[49] Doppler ultrasound in premature infant brain,[50,51] fluorescent microsphere measurement of cerebral blood flow in piglet brain,[38] ASL-MRI in human brain and skeletal muscle,[37,45] and to other reports in the literatures.[30,31,48] DCS flow-oximeter measurements of blood oxygenation in skeletal muscles have been validated against a commercial tissue oximeter (Imagent, ISS Inc., IL, USA).[43]

The purpose of the present study is to test the feasibility of using the novel DCS flow-oximeter for continuous monitoring of both blood flow and oxygenation changes in ischemic muscles during arterial revascularization. Quantification of muscle hemodynamic changes during revascularization would allow us to directly evaluate the acute effects of macro-revascularization in large arteries of upper leg/body on muscle microvasculature/tissues of lower leg, providing a potential for objective assessment of intervention success. For this purpose, we specifically designed fiber-optic probes that can be sterilized and used on patients with PAD undergoing revascularization. These optical probes were taped on the top of medial gastrocnemius (calf) muscles in both legs and connected to the DCS flow-oximeter devices. Muscle hemodynamic changes throughout the entire revascularization procedure were successfully measured and quantified. To the best of our knowledge, there have been no published reports of simultaneous measurements of blood flow and oxygenation in ischemic muscles during revascularization. The ability to continuously and simultaneously monitor multiple hemodynamic parameters could result in deeper insights about the intervention pathology compared to the measurement of a single parameter.

2 Methods

2.1 DCS Tissue Flow-Oximeter

We used a recently developed dual-wavelength four-detection-channel DCS flow-oximeter[43] to continuously monitor blood flow and oxygenation in calf muscles during revascularization. The DCS flow-oximeter, shown in Figs. 1(a) and 1(b), consists of two continual-wave laser diodes with long coherence length (> 5 m) at wavelengths of 785 nm (100 mW) and 854 nm (120 mW) (Crystalaser Inc., NV, USA), four single-photon-counting avalanche photodiodes (APDs, Pacer Components Inc., UK), and a four-channel autocorrelator board (correlator.com, NJ, USA). The two laser diodes work sequentially (on/off) with transistor-transistor logic control signals generated by a digital I/O board (NI Corp., TX, USA), whereas the four APDs operate in parallel. The data acquisition time is ∼2 s (1 s for each wavelength).

Details about the principle of DCS flow-oximeter can be found elsewhere.[43] Briefly, long-coherence NIR light from the two lasers enters the tissue through two multimode source fibers (S1 and S2, diameter = 200 μm). Single-mode detector fibers (D1 and D2, diameter = 5.6 μm) connected to the APDs are used to collect photons from a single speckle emitted from the tissue surface [see Figs. 1(c) and 1(d)]. The light intensity

Table 1 Patient characteristics (boldface rows: patients undergoing PTA; non-bold rows: patients undergoing bypass).

Patient #	Age	Gender	Body Mass Index (BMI)	Surgical procedure
1	**70**	**F**	**30.1**	**Left iliac stent (PTA)**
2	60	F	22.5	Aortobifemoral bypass
3	61	F	27.7	Right femoropopliteal bypass
4	58	M	16.8	Right femoropopliteal bypass
5	73	F	23.6	Left iliofemoral bypass
6	64	F	19.4	Aortobifemoral bypass
7	58	M	20.8	Left iliofemoral bypass
8	59	M	23.8	Femorofemoral bypass & left femoropopliteal bypass
9	**50**	**F**	**35.6**	**Right iliac stent (PTA)**
10	**71**	**F**	**26.0**	**Left iliac stent & profundaplasty (PTA)**
11	**58**	**M**	**27.6**	**Abdominal aorta & both iliac arteries stent (PTA)**

fluctuations within a single speckle area of tissue (~25 μm^2), detected by the APDs, are sensitive to the motions of tissue scatterers (i.e., moving red blood cells). The autocorrelator takes the output of APDs and computes the light intensity autocorrelation function. From the normalized light intensity autocorrelation function, the electric field temporal autocorrelation function $G_1(\tau)$ is derived, which satisfies the correlation diffusion equation in highly scattering media.[52,53] The exact form of the correlation diffusion equation depends on the nature and heterogeneity of the scatterer motion. For the case of diffusive motion, the normalized electric field temporal function $g_1(\tau)$ decays approximately exponentially with the delay time τ when τ is small (e.g., $\tau < 10^{-4}$ s). Blood flow information is extracted by fitting the averaged autocorrelation curve whose decay rate depends on a parameter α (which is proportional to the tissue blood volume fraction) and on the motion of red blood cells.[14,30,47,52] The two wavelengths (785 and 854 nm) generate two flow curves. We have found that DCS flow signals from calf muscles are not sensitive to variation in wavelength.[43]

The oxygenation information is extracted by recording the average detected light intensities at two wavelengths ($\lambda_1 = 785$ and $\lambda_2 = 854$ nm). The wavelengths were chosen based on the lasers available, and optimization of wavelengths[17] will be the subject of future work. The changes of oxygenated hemoglobin concentration ($\Delta[HbO_2]$) and deoxygenated hemoglobin concentration ($\Delta[Hb]$) relative to their baseline values, respectively, (determined before physiological changes) are calculated based on the modified Beer-Lambert Law[17,20]

$$\Delta[HbO_2] = \frac{\varepsilon_{Hb}(\lambda_1)\Delta\mu_a(\lambda_2) - \varepsilon_{Hb}(\lambda_2)\Delta\mu_a(\lambda_1)}{\varepsilon_{Hb}(\lambda_1)\varepsilon_{HbO_2}(\lambda_2) - \varepsilon_{HbO_2}(\lambda_1)\varepsilon_{Hb}(\lambda_2)},$$

$$\Delta[Hb] = \frac{\varepsilon_{HbO_2}(\lambda_2)\Delta\mu_a(\lambda_1) - \varepsilon_{HbO_2}(\lambda_1)\Delta\mu_a(\lambda_2)}{\varepsilon_{Hb}(\lambda_1)\varepsilon_{HbO_2}(\lambda_2) - \varepsilon_{HbO_2}(\lambda_1)\varepsilon_{Hb}(\lambda_2)}$$

Here $\Delta\mu_a(\lambda) = \ln(I_{\lambda B}/I_{\lambda T})/(d \cdot DPF_\lambda)$,[16] where $\Delta\mu_a(\lambda)$ is the relative change of the tissue absorption coefficient at

wavelength λ. $\varepsilon_{HbO_2}(\lambda)$ and $\varepsilon_{Hb}(\lambda)$ are the extinction coefficients of oxy- and deoxy-hemoglobin. $I_{\lambda B}$ and $I_{\lambda T}$ are the measured light intensities at baseline and time T, respectively. DPF_λ (differential pathlength factor) is the ratio of the mean photon pathlength to the distance (d) between the source and detector pair. The DPF primarily depends on the tissue optical properties, which were determined based on the literature.[18] The following values were used in our data analysis:[18,54] $\varepsilon_{HbO2}(785$ nm$) = 1.798$(cm $\cdot$ mM)$^{-1}$, $\varepsilon_{HbO2}(854$ nm$) = 2.584$(cm $\cdot$ mM)$^{-1}$, $\varepsilon_{Hb}(785$nm$) = 2.3$(cm $\cdot$ mM)$^{-1}$, $\varepsilon_{Hb}(854$ nm$) = 1.814$ (cm $\cdot$ mM)$^{-1}$, $DPF_{785\,nm} = 5.56$, and $DPF_{854\,nm} = 5.17$.

2.2 Patient Characteristics

The studies were approved by the Institutional Review Board (IRB) at the University of Kentucky (UK) and took place at the UK Medical Center. With signed IRB consent forms, a total of 12 limbs in 11 patients that underwent vascular reconstructive procedures were studied. Since the major purpose of this study was to test the feasibility of optical techniques for monitoring various revascularizations, we recruited patients mainly based on their willingness to participate in the study (not based on the type of surgical procedures). Table 1 summarizes patient demographics and corresponding surgical procedures. The patients are numbered in a chronological order of surgery date.

2.3 Surgical Procedures

All surgical procedures (see Table 1) were performed by one surgeon (S.S.). The eleven patients can be classified into two groups based on the surgical procedures listed in Table 1: bypass graft (patients #2 to #8, n = 7) and PTA (patient #1 and patients #9 to #11, n = 4). Note that patient #6 underwent aortofemoral bypass on both legs and the data from patient #4 is excluded due to poor installation of the optical probes.

Table 2 Symptomatic and functional improvements after revascularization (boldface rows: patients undergoing PTA; non-bold rows: patients undergoing bypass).

Patient #	Leg	ABI			Fontaine classification of PAD		
		Pre-ABI	Post-ABI	Days obtaining post-ABI after surgery	Pre-surgery	Post-surgery	Days obtaining post-Fontaine class after surgery
1	**L**	**0.24**	**0.27**	**181**	**III**	**I**	**29**
2	L	0.60	n/a	n/a	IIa	I	20
3	R	0.61	0.93	108	IIa	I	108
4	R	0.62	0.92	33	IIa	I	18
5	L	0.78	1.19	61	III	I	13
6	L	n/a	1.02	129	III	IIa	30
	R	n/a	1.06	129			
7	L	0.54	1.02	209	III	IIa	18
8	L	0.69	n/a	n/a	III	IIa	27
9	**R**	**0.62**	**0.66**	**97**	**III**	**IIa**	**20**
10	**L**	**0.53**	**0.87**	**123**	**III**	**IIa**	**17**
11	**L**	**0.62**	**n/a**	**n/a**	**IIb**	**I**	**13**

The patients were placed under general anesthesia. For bypass surgery, the femoral artery was exposed through a sharp vertical incision. During the replacement of the clogged vessel, the femoral artery was temporarily clamped until a bypass graft was in place. For PTA, a micropuncture needle was used to access the femoral artery. A balloon expandable stent was inserted into the clogged artery. The balloon was inflated to compress plaque against the vessel wall and was then removed. The PTA was guided by the repeated x ray angiogram.

2.4 Pre- and Postoperative Evaluations

The patient's pre- and postoperative evaluations included clinical examination (e.g., inspection of feet, palpation of pedal pulse) and noninvasive assessment of PAD using ABI, pulse volume recording, duplex ultrasound scanning, and a walking distance test.[55–57] CT angiography was only used for localization of occluded vessels before operation.

The four-class Fontaine classification system[58] was used for symptomatic classification of PAD before and after revascularization (see Table 2), in which, Stage I: ABI < 0.9 with mild pain when walking; Stage IIa: severe pain with IC when walking relatively longer distances (> 200 m); Stage IIb: severe pain with IC when walking relatively shorter distances ($\leq$ 200 m); Stage III: pain while resting; Stage IV: biological tissue loss.

2.5 Optical Measurement Protocol

All patients underwent the assessment of blood flow and oxygenation in their medial gastrocnemius (calf) muscles using the DCS flow-oximeter. A fiber-optic probe [see Figs. 1(c)

and 1(d)] was sterilized using a low temperature oxidative sterilization method (STERRAD™, Advanced Sterilization Products, CA, USA). The sterilized probe was taped to the surfaces of medial gastrocnemius muscles in the operated legs (n = 12) before surgery using sterile transparent dressing (Tegaderm™, 3M Health Care, MN, USA). For comparison, another fiber-optic probe was taped to the surfaces of calf muscles in the untreated (control) legs of four patients (patients #8 to #11). The two probes were connected to two DCS flow-oximeter devices through long optical fibers (length = 5 m). The portable optical devices sat at the bedside in the operating room without interrupting surgical procedures. Calf muscle blood flow and oxygenation were continuously monitored throughout the entire revascularization procedure.

2.6 Optical Data Analysis

Skin and adipose tissue layers generally lie above the medial gastrocnemius muscles and might influence the optical measurements of muscle hemodynamics. In this study, data derived from the larger source-detector separation (2.5 cm) are used to quantify tissue blood flow and oxygenation in deep calf muscles, as the light penetration depth is proportional to the separation (approximately one-half of the separation).[14, 46] According to multi-layer models of diffusion theory[59–61] and our previous studies,[14, 43] the signals detected by this separation (2.5 cm) mainly derive from the calf muscles in subjects with regular thickness of top tissue layers. Since the body-mass-indices [24.9 $\pm$ 1.6 kg/m^2 (mean $\pm$ standard error)] of the patients that we measured fall in the normal range,[62, 63]
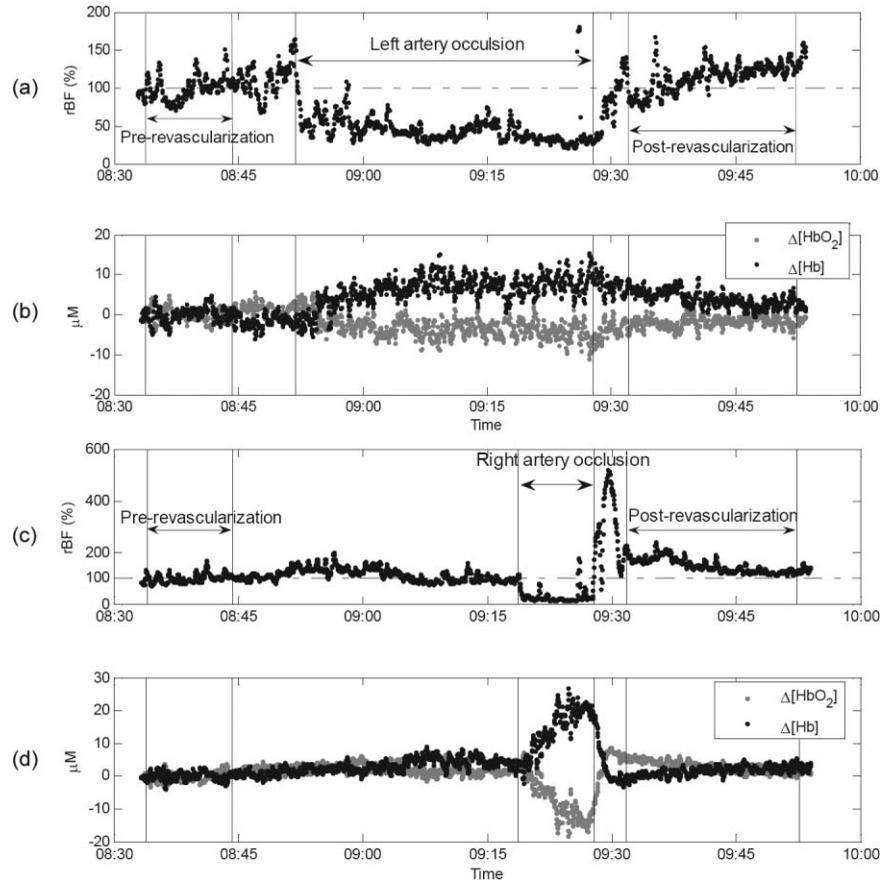
Fig. 2 Typical muscle hemodynamic responses during Bi-femoral artery bypass graft in patient #6; (a) rBF in left calf muscle. (b) $\Delta[HbO_2]$ and $\Delta[Hb]$ in left calf muscle, (c) rBF in right calf muscle. (d) $\Delta[HbO_2]$ and $\Delta[Hb]$ in right calf muscle. The vertical lines indicate the beginning and ending of temporary arterial clamps or the periods for calculation of the pre-revascularization baseline (10 min) and post-revascularization value (20 min). The time courses of DCS data were normalized (divided) by the averaged 10-min pre-revascularization baseline (assigned 100%) for the calculation of rBF. During the clamping of the femoral artery (left or right), muscle rBF in the clamped leg significantly decreased (a and c), causing a gradual decrease/increase in $\Delta[HbO_2]/\Delta[Hb]$ (b and d) in the clamped leg. The opposite unclamped leg did not show much hemodynamic change during the arterial clamping of the operated leg. When the bi-arterial clamps were released, both legs clearly showed reactive hyperemia (hemodynamic overshoot). The post-bypass rBF (a and c) were higher than their baselines while the post-bypass $\Delta[HbO_2]$ and $\Delta[Hb]$ (b and d) were recovered to their baseline levels, respectively.

the NIR light can penetrate through the top tissue layers into the calf muscles. Note, however, even at this relatively large source-detector separation, there is always some contribution to the signal from the overlaying tissues.

Since DCS flow signals are not sensitive to variation in wavelength,[43] in this study we present flow data of only one wavelength (785 nm). Following the method used in many previous studies for quantification of blood flow changes,[14,37,43,45,46,64] the rBF is defined as the percentage change relative to its baseline value that is assigned to be 100% or 1. The mean values of hemodynamic data during arterial clamping and during balloon inflation are respectively calculated and compared to their baselines for evaluating the influence of arterial manipulations on muscle hemodynamics. Note that some patients were subjected to multiple arterial clamps during bypass surgery or multiple balloon inflations during PTA. In these cases, hemodynamic data during multiple clamps/inflations are averaged. To characterize the acute post-revascularization effect in muscle hemodynamics, post-revascularization data are averaged for 20 min and compared to the averaged 10-min pre-revascularization baselines (see Figs. 2 and 3). For eval-

uation of the average effect over subjects, mean and standard error (SE) are calculated and plotted (see Figs. 4–6). Significant differences are identified by paired t-tests, where the criterion for significance is $p < 0.05$.

3 Results

3.1 *Individual Muscle Hemodynamic Change During Revascularization*

The calf muscle hemodynamics showed large inter-patient variations during revascularization due to the nature of different surgical procedures in each individual. However, the patients can be classified into two groups based on the surgical procedures listed in Table 1: bypass graft and PTA.

3.1.1 *Typical bypass response*

Figure 2 shows typical calf muscle hemodynamic responses in both legs of patient #6 who underwent an aortofemoral bypass on both legs. The surgery for this patient was performed as follows. The common femoral arteries (CFA) and their divisions
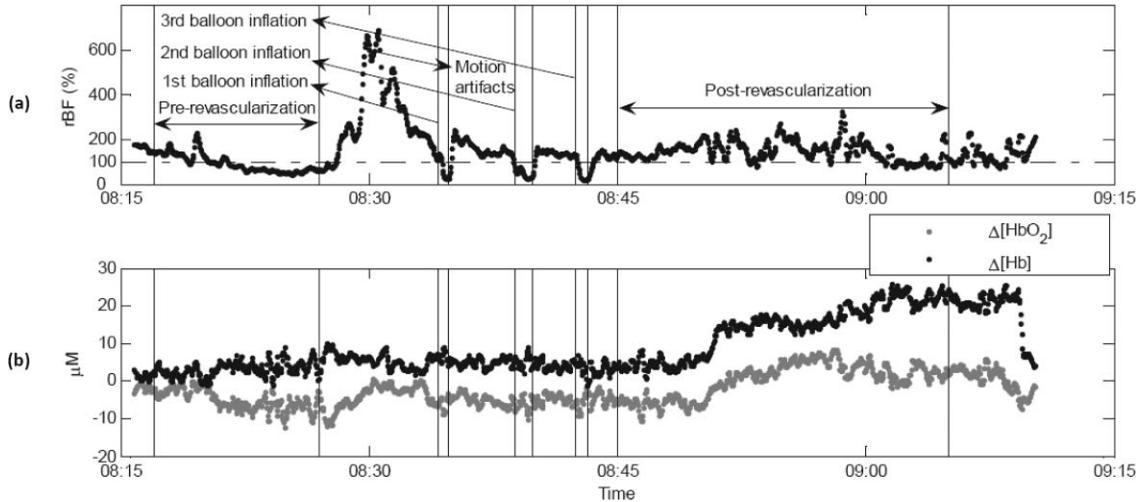
Fig. 3 Typical calf muscle responses in (a) rBF and (b) $\Delta[HbO_2]$ and $\Delta[Hb]$ during iliac arterial PTA in patient #1. The vertical lines indicate the beginning and ending of balloon inflations or the periods for calculation of the pre-revascularization baseline (10 min) and post-revascularization values (20 min). The time courses of DCS data were normalized (divided) by the averaged 10-min pre-revascularization baseline (assigned 100%) for the calculation of rBF. (a) The rBF decreased during the balloon inflations in the operated leg, whereas (b) no obvious changes in $\Delta[HbO_2]$ and $\Delta[Hb]$ were observed. The post-PTA rBF was higher than its baseline value. The post-PTA rBF increase caused increases in both $[HbO_2]$ and $[Hb]$ in this patient, indicating an increase in blood volume (proportional to the total hemoglobin concentration: sum of $[HbO_2]$ and $[Hb]$). Note that there was a large motion artifact in optical measurements around the time of 08:30 am when the patient's position was adjusted for the convenience of surgical operation.

were exposed through a sharp vertical incision in each groin. The abdomen was opened through a midline incision. First, proximal anastomosis was made with the aorta as end to side fashion. Each limb of the graft was then anastomosed to the CFA; first to the left then to the right side. The femoral arteries (left and right) were clamped sequentially during the replacement of the occluded vessels. Blood flow was then restored by releasing the vascular clamps.

When the femoral artery (left or right) was sequentially clamped, calf muscle rBF in the clamped leg significantly decreased [see Figs. 2(a) and 2(c)], causing a gradual decrease in $\Delta[HbO_2]$ and a gradual increase in $\Delta[Hb]$ [see Figs. 2(b) and 2(d)] in the clamped leg. As expected, the opposite unclamped leg did not show much hemodynamic change during the clamping of the operated leg.

When the arterial clamps (left and right) were released, immediate reactive hyperemia responses were observed (i.e., the overshoots in rBF, $\Delta[HbO_2]$ and $\Delta[Hb]$) in both legs. After the completion of entire bypass in both legs, the post-bypass rBF were higher than their baselines, and the post-bypass $\Delta[HbO_2]$ and $\Delta[Hb]$ were recovered gradually to their pre-bypass baseline levels.
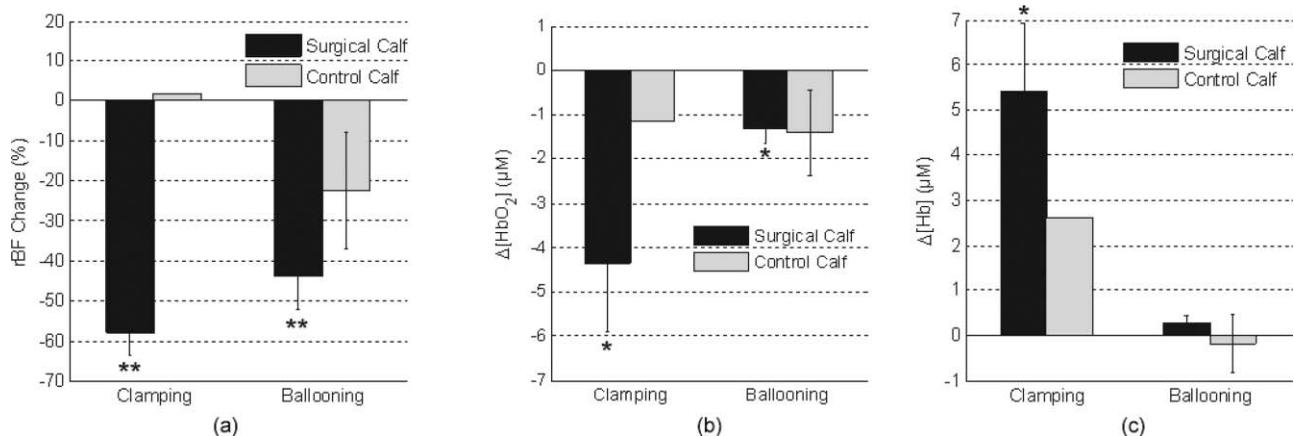
Fig. 4 Average changes (mean $\pm$ SE) in (a) blood flow, (b) $\Delta[HbO_2]$, and (c) $\Delta[Hb]$ of calf muscles during arterial clamping ($n = 7$) and balloon inflation ($n = 4$). Significant decreases in calf blood flow (rBF) were observed during both arterial clamping and balloon inflation in the operated legs. The long-period arterial clamps during bypass procedure caused relatively large deoxygenation (decrease/increase in $\Delta[HbO_2]/\Delta[Hb]$) in calf muscles whereas the short-period balloon inflations during PTA induced small changes in tissue oxygenation. Muscle hemodynamic changes in the control legs ($n = 4$) varied remarkably and did not show a consistent pattern. * ($p < 0.05$) and ** ($p < 0.01$) represent significant differences compared to the baseline value.
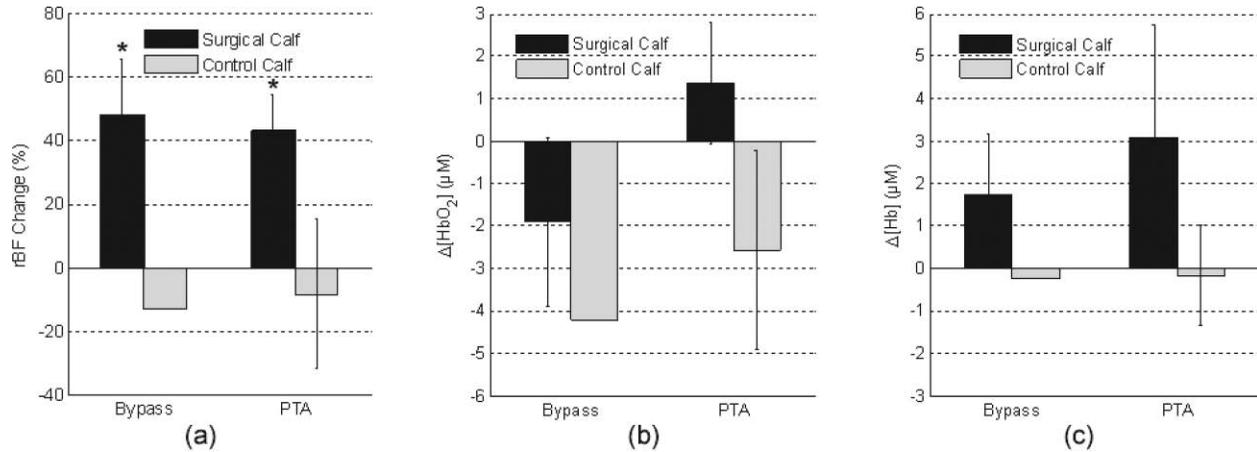
Fig. 5 Average changes (mean $\pm$ SE) in (a) blood flow, (b) $\Delta[HbO_2]$, and (c) $\Delta[Hb]$ of calf muscles after bypass and PTA. Significant increases in calf blood flow (rBF) were found in patients with bypass graft (n = 7) and PTA (n = 4) compared to the pre-revascularization values, respectively. Acute post-revascularization effects in calf oxygenation ($\Delta[HbO_2]$ and $\Delta[Hb]$) were not evident for both bypass and PTA. Muscle hemodynamic changes in the control legs (n = 4) varied remarkably and did not show a consistent pattern. * (p < 0.05) represents significant difference compared to the baseline value.

3.1.2 Typical PTA response

Figure 3 shows the typical calf muscle hemodynamic responses during iliac arterial PTA in patient #1. The surgery for this patient was performed as follows. A micropuncture needle was used to access the left CFA. A 7×37 mm balloon expandable stent was inserted into the stenosis of external iliac artery at the junction of the hypogastricon on the left side. The balloon was inflated three times to compress plaque against the vessel wall and was then removed. The PTA was guided by the repeated x ray angiogram.

The calf muscle rBF significantly decreased during the balloon inflations (three times) in the operated leg [see Fig. 3(a)], whereas no obvious changes in $\Delta[HbO_2]$ and $\Delta[Hb]$ were observed during the short-period inflations/deflations [see Fig. 3(b)]. As expected, the immediate reactive hyperemia responses were much smaller after the short-period inflations/deflations compared to those observed in patient #6 after release of long-period arterial clamping. Similar to the post-bypass rBF response observed in patient #6, the post-PTA rBF was higher than its baseline value.

3.2 Average Results Over Subjects

3.2.1 During revascularization

Figure 4 shows the average hemodynamic responses during arterial clamping/balloon inflation from all patients except patient #4 (optical data from this patient is not available due to poor installation of the optical probe). Although large inter-patient variation existed, the patients exhibited consistent hemodynamic response patterns during revascularization in the surgical legs. On average, significant decreases in calf rBF were observed [see Fig. 4(a)] during arterial clamping ($-57.9 \pm 5.5\%$, n = 7, $p = 4.5 \times 10^{-5}$) and during balloon inflation ($-44.0 \pm 7.4\%$, n = 4, p = 0.009) in the surgical legs. As expected, the long-period [ranged from 7.8–58.0 (22.1 $\pm$ 6.9) min] arterial clamps during bypass procedure caused relatively large deoxygenation ($\Delta[HbO_2] = -4.3 \pm 1.6 \mu$Mol, $\Delta[Hb] = +5.4 \pm 1.5 \mu$Mol, n = 7, p < 0.05) in calf muscles whereas the short-period

(several seconds) balloon inflations during PTA induced small changes ($\Delta[HbO_2] = -1.3 \pm 0.3 \mu$Mol, $\Delta[Hb] = +0.3 \pm 0.1 \mu$Mol, n = 4) in tissue oxygenation [see Figs. 4(b) and 4(c)]. Note, however, that the small number of patients/measurements may affect the power for the test of statistical significance.

By contrast, muscle hemodynamic changes in the control legs (n = 4) varied remarkably (see Fig. 4) and did not show a consistent pattern as the individual surgical procedure may or may not affect the contralateral control leg. In fact, three out of four control legs (patients #8, #10, #11) were affected by the surgical procedures (see Table 1). For example, patient #10 was found to have lesion at the distal aorta above the bifurcation during the PTA procedure. A balloon was then inflated and stent was deployed at the distal aorta, which temporarily affected blood flow to both legs. Similarly, calf blood flow in both legs was influenced by the femoral-femoral bypass graft deployed in patient #8 and by the abdominal aorta stent deployed in patient #11.

3.2.2 Post revascularization

Figure 5 shows the average post-revascularization responses in calf muscle hemodynamics. The post-revascularization hemodynamic responses in calf muscles after the two different operative procedures (bypass graft and PTA) were similar. Significant elevations in calf rBF were found in the surgical legs after bypass graft ($+48.1 \pm 17.5\%$, n = 7, p = 0.03) and after PTA ($+43.2 \pm 11.0\%$, n = 4, p = 0.03), compared to the pre-revascularization values, respectively. Acute post-revascularization effects in calf oxygenation were not evident for both bypass graft ($\Delta[HbO_2] = -1.9 \pm 2.0 \mu$Mol, $\Delta[Hb] = +1.8 \pm 1.4 \mu$Mol, n = 7, p > 0.05) and PTA ($\Delta[HbO_2] = +1.4 \pm 1.4 \mu$Mol, $\Delta[Hb] = +3.1 \pm 2.7 \mu$Mol, n = 4, p > 0.05). Similarly to the responses during revascularization, muscle hemodynamic responses after revascularization did not show a consistent pattern in the control legs.

Most patients showed significant short-term symptomatic improvements (see the changes in Fontaine classification stages) with increases of ABI after revascularization, as listed in

Table 2. The post-revascularization stages of Fontaine classification and post-ABIs were measured 13~108 (28 ± 26) and 33~209 (119 ± 54) days after revascularization, respectively. It would be ideal to obtain these measurements within the same period of time after surgery for the comparison of individual post-revascularization improvements. However, the patients involved in this study live within a broad geographic region and cannot walk for a long distance due to PAD. This makes the follow-up hospital visit difficult, leading to a large variation among patients in days after surgery for implementing these evaluations. Importantly, the short-term symptomatic and functional improvements after revascularization were associated with the acute post-revascularization flow elevations/improvements in calf muscles. Figure 6 shows the significant changes in both ABI (ΔABI = +0.23 ± 0.08, p = 0.04) and rBF (ΔrBF = +0.29 ± 0.08, p = 0.02; assigning a pre-revascularization baseline rBF = 1) from the six patients (three bypass and three PTA) whose ΔABIs and optical data were available (see Table 2). Notice that about half of the patients did not have a complete ABI test result (i.e., lack of pre- and/or post-ABI) due to their absence from the scheduled examinations. Since the patients with different surgical procedures (bypass or PTA) showed similar post-revascularization hemodynamic responses (see above), the data from these six patients were not separated based on their surgical procedures for this comparison (see Fig. 6). However, no significant correlation was found between the changes of rBF and ABI in these six patients.

4 Discussion and Conclusions

The goal of arterial revascularization in patients with PAD is to reestablish large arterial blood supply to ischemic tissues in the lower leg muscles. It is thus crucial to evaluate the hemodynamic changes/improvements in lower leg muscles during and after the revascularization. Currently no gold standard for this evaluation is available, as the clinical presentation is a derivative of a combination of flow, tissue oxygenation, oxygen extraction, and utilization.[26] We have shown in this study that muscle hemodynamic changes (including both blood flow and oxygenation) during revascularization can be detected by the NIR diffuse optical technology (DCS flow-oximeter, see Fig. 1) that we recently developed. The optical technology has important advantages over one-time imaging modalities (e.g., MRI, x ray/CT) in terms of being noninvasive, fast, continuous, portable, and inexpensive.

The optical measurements demonstrate the capability to continuously monitor hemodynamic changes during different revascularization operations. During bypass surgery, with the clamping of femoral artery for a long period of time, a significant decrease in blood flow was found to be associated with significant deoxygenation in the calf muscles (see Figs. 2 and 4). After release of the arterial clamping, an immediate increase/recovery in blood flow and oxygenation (reactive hyperemia) was observed. These hemodynamic responses during revascularization are similar to those in calf muscles during thigh arterial cuff occlusion/releasing previously observed.[14,43] This consistence is anticipated since both arterial occlusion (during cuff occlusion) and arterial clamping (during bypass) shut off the blood supply to the lower leg. Furthermore, the clamping/releasing-induced
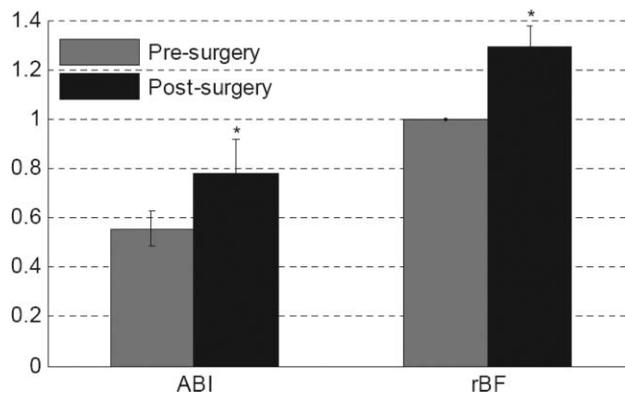

Fig. 6 ABI and rBF (mean ± SE) before and after revascularization in six patients (three bypass and three PTA) whose ΔABIs and optical data were available. The post-revascularization rBF data were averaged for 20 min and compared to the averaged 10-min pre-revascularization baselines (assigned 1). The short-term ABI improvements (ABI increases at 33~209 days after surgery compared to its pre-surgery value) were associated with the acute post-revascularization flow improvements (rBF immediately increases after surgery compared to its pre-surgery value) in the calf muscles of the surgical legs. * (p < 0.05) represents significant difference between the mean values of pre-surgery and post-surgery.

deoxygenation/reoxygenation is similar to the oxygenation response during HA bypass surgery observed in others' study.[3]

During PTA, with a temporal resolution of ~0.5 Hz, DCS flow-oximeter can detect rapid changes in calf rBF induced by short-period (several seconds) balloon inflations and deflations [see Figs. 3 and 4(a)]. As expected, the short-period perturbations in blood supply (rBF) did not cause large changes in [HbO$_2$] and [Hb] [see Figs. 3, 4(b) and 4(c)]. In total, the anticipated muscle hemodynamic variations during bypass surgery and during PTA verify the capability of DCS flow-oximeter for monitoring dynamic physiological events during revascularization.

Noninvasive quantification of post-revascularization effects in muscle hemodynamics is the major goal of this study. We found in this study that the repairs of the macro-circulation by both bypass graft and PTA resulted in similar post-revascularization responses in calf muscle hemodynamics. Acute blood flow elevations in calf muscles were observed within 20 min after bypass graft and PTA [see Fig. 5(a)]. The post-bypass rBF elevation may result from the reestablishment of large arterial blood supply to the ischemic muscle as well as the reperfusion after temporary arterial clamping. By contrast, the post-PTA rBF elevations are solely due to the muscle blood flow improvements after arterial revascularization since there was no obvious reactive hyperemia/reperfusion after the short-period arterial inflations.

In contrast to the acute elevation/improvement in muscle blood flow after revascularization, there was no acute post-revascularization improvement in muscle blood oxygenation [see Figs. 5(b) and 5(c)], which is consistent with the oxygenation measurement results immediately after HA bypass surgery.[3] Although clarification of the reasons for limited acute tissue oxygenation changes requires separate investigations, it is possible that the acute rBF increase may have been balanced by an increase in tissue oxygen utilization immediately after

revascularization. The decoupling of muscle blood flow and blood oxygenation after revascularization emphasizes the need for simultaneous monitoring of both parameters.

The acute post-revascularization flow elevation /improvements in surgical calf muscles were associated with the short-term symptomatic and functional improvements after revascularization (see Table 2). For example, the averaged results from the six patients (see Fig. 6) showed similar percentage changes in both rBF ($+29\%$) and ABI ($+23\%$). However, our present results did not show a significant correlation between the acute rBF changes after revascularization and the short-term ABI improvements. It is possible that the lack of statistical correlation may be due to the small number of patients (n = 6).

Previous studies have compared angiographically graded coronary blood flow with intracoronary Doppler flow velocity in patients during percutaneous transluminal coronary angioplasty for acute myocardial infarction.[65] Improved blood flow grades after the reperfusion therapy have been associated with improved clinical results. Determination of blood flow level after coronary reperfusion yielded important prognostic information in patients with acute myocardial infarction.[65–67] Based on these observations, one would expect that hemodynamic measurements in ischemic muscle during and after revascularization should generate prognostic information for long-term treatment outcomes. To test the prognostic value of optical techniques in evaluating arterial revascularization, however, a large patient population with longitudinal measurements is needed to correlate the acute/short-term (i.e., during/days or weeks after revascularization) hemodynamic improvements with long-term (i.e., months or years after revascularization) symptomatic and functional improvements. A large patient pool would also increase the statistical power of measurement results. It would also be interesting to explore the "absolute" baseline measurement of muscle hemodynamics before surgical procedure for predicting the success of arterial revascularization. Such investigations are the subject of our future work. Other improvements in future study should include recruiting patients more evenly based on the surgical procedures (e.g., bypass graft versus PTA) and collecting complete ABI and control data from all patients.

To conclude, this study demonstrates that the novel portable DCS flow-oximeter can be used for continuous monitoring and quantitative evaluation of acute revascularization effects in muscle hemodynamics at the bedside of operating rooms. This optical device probes multiple hemodynamic parameters (i.e., rBF, $\Delta[\text{HbO}_2]$, $\Delta[\text{Hb}]$) without the needs of contrast agents and venous occlusions, which is particularly crucial for continuous intraoperative monitoring of arterial revascularization. Simultaneous measurements of multiple hemodynamic parameters during and after revascularization provide a better understanding about the underlying mechanisms of the surgical interventions, and hold a potential for objectively assessing the success of arterial revascularization.

References

1. J. Feinglass, M. Morasch, and W. J. McCarthy, "Measures of success and health-related quality of life in lower-extremity vascular surgery," *Annu. Rev. Med.* **51**, 101–113 (2000).
2. W. R. Hiatt, "Medical treatment of peripheral arterial disease and claudication," *N. Engl. J. Med.* **344**(21), 1608–1621 (2001).
3. N. Unno, K. Inuzuka, N. Yamamoto, D. Sagara, M. Suzuki, and H. Konno, "Preservation of pelvic circulation with hypogastric artery bypass in endovascular repair of abdominal aortic aneurysm with bilateral iliac artery aneurysms," *J. Vasc. Surg.* **44**(6), 1170–1175 (2006).
4. J. Feinglass, W. J. McCarthy, R. Slavensky, L. M. Manheim, and G. J. Martin, "Functional status and walking ability after lower extremity bypass grafting or angioplasty for intermittent claudication: results from a prospective outcomes study," *J. Vasc. Surg.* **31**(1 Pt 1), 93–103 (2000).
5. M. A. Zatina, H. D. Berkowitz, G. M. Gross, J. M. Maris, and B. Chance, "31P nuclear magnetic resonance spectroscopy: noninvasive biochemical analysis of the ischemic extremity," *J. Vasc. Surg.* **3**(3), 411–420 (1986).
6. M. G. M. Hunink, J. B. Wong, M. C. Donaldson, M. F. Meyerovitz, and D. P. Harrington, "Patency results of percutaneous and surgical revascularization for femoropopliteal arterial-disease," *Med. Decis. Making* **14**(1), 71–81 (1994).
7. R. S. Sawaqed, F. J. Podbielski, H. E. Rodriguez, I. M. Wiesman, M. M. Connolly, and E. T. Clark, "Prospective comparison of intraoperative angiography with duplex scanning in evaluating lower-extremity bypass grafts in a community hospital," *Am. Surg.* **67**(6), 601–604 (2001).
8. L. Balacumaraswami and D. P. Taggart, "Intraoperative imaging techniques to assess coronary artery bypass graft patency," *Ann. Thorac. Surg.* **83**(6), 2251–2257 (2007).
9. M. Jugold, M. Palmowski, J. Huppert, E. C. Woenne, M. M. Mueller, W. Semmler, and F. Kiessling, "Volumetric high-frequency Doppler ultrasound enables the assessment of early antiangiogenic therapy effects on tumor xenografts in nude mice," *Eur. Radiol.* **18**(4), 753–758 (2008).
10. H. Li, B. A. Standish, A. Mariampillai, N. R. Munce, Y. X. Mao, S. Chiu, N. E. Alarcon, B. C. Wilson, A. Vitkin, and V. X. D. Yang, "Feasibility of interstitial Doppler optical coherence tomography for in vivo detection of microvascular changes during photodynamic therapy," *Lasers Surg. Med.* **38**(8), 754–761 (2006).
11. G. B. Yvonne-Tee, A. H. G. Rasool, A. S. Halim, and A. R. A. Rahman, "Noninvasive assessment of cutaneous vascular function in vivo using capillaroscopy, plethysmography and laser-Doppler instruments: its strengths and weaknesses," *Clin. Hemorheol Microcirc* **34**(4), 457–473 (2006).
12. H. U. Volker, G. Roper, J. Sterk, and C. Willy, "Long-term invasive measurement of subcutaneous oxygen partial pressure above the sacrum on lying healthy volunteers," *Wound Repair Regen.* **14**(5), 542–547 (2006).
13. T. Yamada, T. Ohta, H. Ishibashi, I. Sugimoto, H. Iwata, M. Takahashi, and J. Kawanishi, "Clinical reliability and utility of skin perfusion pressure measurement in ischemic limbs–comparison with other noninvasive diagnostic methods," *J. Vasc. Surg.* **47**(2), 318–323 (2008).
14. G. Yu, T. Durduran, G. Lech, C. Zhou, B. Chance, E. R. Mohler, and A. G. Yodh, "Time-dependent blood flow and oxygenation in human skeletal muscles measured with noninvasive near-infrared diffuse optical spectroscopies," *J. Biomed. Opt.* **10**(2), 024027 (2005).
15. S. O. de Vries, K. Visser, J. A. de Vries, J. B. Wong, M. C. Donaldson, and M. G. Hunink, "Intermittent claudication: cost-effectiveness of revascularization versus exercise therapy," *Radiology* **222**(1), 25–36 (2002).
16. S. Fantini, D. Hueber, M. A. Franceschini, E. Gratton, W. Rosenfeld, P. G. Stubblefield, D. Maulik, and M. R. Stankovic, "Non-invasive optical monitoring of the newborn piglet brain using continuous-wave and frequency-domain spectroscopy," *Phys. Med. Biol.* **44**(6), 1543–1563 (1999).
17. G. Strangman, M. A. Franceschini, and D. A. Boas, "Factors affecting the accuracy of near-infrared spectroscopy concentration calculations for focal changes in oxygenation parameters," *Neuroimage* **18**(4), 865–879 (2003).

18. A. Duncan, J. H. Meek, M. Clemence, C. E. Elwell, L. Tyszczuk, M. Cope, and D. T. Delpy, "Optical pathlength measurements on adult head, calf and forearm and the head of the newborn infant using phase resolved optical spectroscopy," *Phys. Med. Biol.* **40**(2), 295–304 (1995).

19. K. K. Mccully, C. Halber, and J. D. Posner, "Exercise-induced changes in oxygen saturation in the calf muscles of elderly subjects with peripheral vascular disease," *J. Gerontol.* **49**(3), B128–B134 (1994).

20. Y. L. Song, J. G. Kim, R. P. Mason, and H. L. Liu, "Investigation of rat breast tumour oxygen consumption by near-infrared spectroscopy," *J. Phys. D: Appl. Phys.* **38**(15), 2682–2690 (2005).

21. D. J. Wallace, B. Michener, D. Choudhury, M. Levi, P. Fennelly, D. M. Hueber, and B. B. Barbieri, "Results of a 95-subject human clinical trial for the diagnosis of peripheral vascular disease using a near-infrared frequency domain hemoglobin spectrometer," in *Proceedings of SPIE*, B. Chance, R. R. Alfano, and B. J. Tromberg, Eds., pp. 300–316, San Jose, CA (1999).

22. T. R. Cheatle, L. A. Potter, M. Cope, D. T. Delpy, P. D. C. Smith, and J. H. Scurr, "Near-infrared spectroscopy in peripheral vascular-disease," *Brit. J. Surg.* **78**(4), 405–408 (1991).

23. H. M. Kooijman, M. T. E. Hopman, W. N. J. M. Colier, J. A. vanderVliet, and B. Oeseburg, "Near infrared spectroscopy for noninvasive assessment of claudication," *J. Surg. Res.* **72**(1), 1–7 (1997).

24. U. Wolf, M. Wolf, J. H. Choi, M. Levi, D. Choudhury, S. Hull, D. Coussirat, L. A. Paunescu, L. P. Safonova, A. Michalos, W. W. Mantulin, and E. Gratton, "Localized irregularities in hemoglobin flow and oxygenation in calf muscle in patients with peripheral vascular disease detected with near-infrared spectrophotometry," *J. Vasc. Surg.* **37**(5), 1017–1026 (2003).

25. A. Paunescu, "Tissue blood flow and oxygen consumption measured with near-infrared frequency-domain spectroscopy," Ph.D. Thesis, University of Illinois, Urbana (2001).

26. M. Vardi and A. Nini, "Near-infrared spectroscopy for evaluation of peripheral vascular disease. A systematic review of literature," *Eur. J. Vasc. Endovasc. Surg.* **35**(1), 68–74 (2008).

27. C. Casavola, L. A. Paunescu, S. Fantini, M. A. Franceschini, P. M. Lugara, and E. Gratton, "Application of near-infrared tissue oxymetry to the diagnosis of peripheral vascular disease," *Clin. Hemorheol Microcirc* **21**(3–4), 389–393 (1999).

28. N. Unno, M. Suzuki, N. Yamamoto, K. Inuzuka, D. Sagara, M. Nishlyama, H. Tanaka, and H. Konno, "Indocyanine green fluorescence angiography for intraoperative assessment of blood flow: a feasibility study," *Eur. J. Vasc. Endovasc. Surg.* **35**(2), 205–207 (2008).

29. L. Gagnon, M. Desjardins, J. Jehanne-Lacasse, L. Bherer, and F. Lesage, "Investigation of diffuse correlation spectroscopy in multilayered media including the human head," *Opt. Express* **16**(20), 15514–15530 (2008).

30. C. Cheung, J. P. Culver, K. Takahashi, J. H. Greenberg, and A. G. Yodh, "In vivo cerebrovascular measurement combining diffuse near-infrared absorption and correlation spectroscopies," *Phys. Med. Biol.* **46**(8), 2053–2065 (2001).

31. G. Dietsche, M. Ninck, C. Ortolf, J. Li, F. Jaillon, and T. Gisler, "Fiber-based multispeckle detection for time-resolved diffusing-wave spectroscopy: characterization and application to blood flow detection in deep tissue," *Appl. Opt.* **46**(35), 8506–8514 (2007).

32. J. P. Culver, T. Durduran, T. Furuya, C. Cheung, J. H. Greenberg, and A. G. Yodh, "Diffuse optical tomography of cerebral blood flow, oxygenation, and metabolism in rat during focal ischemia," *J. Cereb. Blood Flow Metab.* **23**(8), 911–924 (2003).

33. C. Zhou, R. Choe, N. Shah, T. Durduran, G. Yu, A. Durkin, D. Hsiang, R. Mehta, J. Butler, A. Cerussi, B. J. Tromberg and A. G. Yodh, "Diffuse optical monitoring of blood flow and oxygenation in human breast cancer during early stages of neoadjuvant chemotherapy," *J. Biomed. Opt.* **12**(5), 051903 (2007).

34. U. Sunar, H. Quon, T. Durduran, J. Zhang, J. Du, C. Zhou, G. Yu, R. Choe, A. Kilger, R. Lustig, L. Loevner, S. Nioka, B. Chance and A. G. Yodh, "Noninvasive diffuse optical measurement of blood flow and blood oxygenation for monitoring radiation therapy in patients with head and neck tumors: a pilot study," *J. Biomed. Opt.* **11**(6), (2006).

35. J. Li, M. Ninck, L. Koban, T. Elbert, J. Kissler, and T. Gisler, "Transient functional blood flow change in the human brain measured noninvasively by diffusing-wave spectroscopy," *Opt. Lett.* **33**(19), 2233–2235 (2008).

36. T. Durduran, C. Zhou, B. L. Edlow, G. Yu, R. Choe, M. N. Kim, B. L. Cucchiara, M. E. Putt, Q. Shah, S. E. Kasner, J. H. Greenberg, A. G. Yodh and J. A. Detre, "Transcranial optical monitoring of cerebrovascular hemodynamics in acute stroke patients," *Opt. Express* **17**(5), 3884–3902 (2009).

37. T. Durduran, G. Yu, M. G. Burnett, J. A. Detre, J. H. Greenberg, J. J. Wang, C. Zhou, and A. G. Yodh, "Diffuse optical measurement of blood flow, blood oxygenation, and metabolism in a human brain during sensorimotor cortex activation," *Opt. Lett.* **29**(15), 1766–1768 (2004).

38. C. Zhou, S. A. Eucker, T. Durduran, G. Yu, J. Ralston, S. H. Friess, R. N. Ichord, S. S. Margulies, and A. G. Yodh, "Diffuse optical monitoring of hemodynamic changes in piglet brain with closed head injury," *J. Biomed. Opt.* **14**(3), 034015 (2009).

39. G. Maret and P. E. Wolf, "Multiple light-scattering from disordered media – the effect of brownian-motion of scatterers," *Z. Phys. B: Condens. Matter* **65**(4), 409–413 (1987).

40. D. J. Pine, D. A. Weitz, P. M. Chaikin, and E. Herbolzheimer, "Diffusing-wave spectroscopy," *Phys. Rev. Lett.* **60**(12), 1134–1137 (1988).

41. M. Belau, M. Ninck, G. Hering, and T. Gisler, "Non-invasive measurement of skeletal muscle contraction with time-resolved diffusing-wave spectroscopy," in *Conference on Biomedical Optics and 3D Imaging*, p. paper BSuD70, Technical Digest (CD) (Optical Society of America, 2010), Miami, FL, USA (2010).

42. Y. Shang, Y. Zhao, R. Cheng, L. Dong, D. Irwin, K. R. Swartz, S. S. Salles, and G. Yu, "Diffuse optical spectroscopies for evaluation of muscle hemodynamic enhancements by electrical stimulation," in Conference on Biomedical Optics and 3D Imaging, p. paper BSuD80, Technical Digest (CD) (Optical Society of America, 2010), Miami, FL, USA (2010).

43. Y. Shang, Y. Zhao, R. Cheng, L. Dong, D. Irwin, and G. Yu, "Portable optical tissue flow oximeter based on diffuse correlation spectroscopy," *Opt. Lett.* **34**(22), 3556–3558 (2009).

44. X. Xing, E. R. Mohler, C. Zhou, T. Durduran, G. M. Lech, Y. Shi, R. Wilensky, J. Moore, A. G. Yodh, and G. Yu, "Hemodynamic changes in diabetic pig muscle," in SVMB 18th Annual Meeting, Baltimore, MA (2007).

45. G. Yu, T. F. Floyd, T. Durduran, C. Zhou, J. J. Wang, J. A. Detre, and A. G. Yodh, "Validation of diffuse correlation spectroscopy for muscle blood flow with concurrent arterial spin labeled perfusion MRI," *Opt. Express* **15**(3), 1064–1075 (2007).

46. Y. Shang, T. B. Symons, T. Durduran, A. G. Yodh, and G. Yu, "Effects of muscle fiber motion on diffuse correlation spectroscopy blood flow measurements during exercise," *Biomed. Opt. Express* **1**(2), 500–511 (2010).

47. G. Yu, T. Durduran, C. Zhou, H. W. Wang, M. E. Putt, H. M. Saunders, C. M. Sehgal, E. Glatstein, A. G. Yodh, and T. M. Busch, "Noninvasive monitoring of murine tumor blood flow during and after photodynamic therapy provides early assessment of therapeutic efficacy," *Clin. Cancer. Res.* **11**(9), 3543–3552 (2005).

48. T. Durduran, "Non-invasive measurements of tissue hemodynamics with hybrid diffuse optical methods," Ph.D. Thesis, University of Pennsylvania, Philadelphia (2004).

49. M. N. Kim, T. Durduran, S. Frangos, B. L. Edlow, E. M. Buckley, H. E. Moss, C. Zhou, G. Yu, R. Choe, E. Maloney-Wilensky, R. L. Wolf, M. S. Grady, J. H. Greenberg, J. M. Levine, A. G. Yodh, J. A. Detre and W. A. Kofke, "Noninvasive measurement of cerebral blood flow and blood oxygenation using near-infrared and diffuse correlation spectroscopies in critically brain-injured adults," *Neurocrit. Care* **12**(2), 173–180 (2010).

50. E. M. Buckley, N. M. Cook, T. Durduran, M. N. Kim, C. Zhou, R. Choe, G. Yu, S. Shultz, C. M. Sehgal, D. J. Licht, P. H. Arger, M. E. Putt, H. Hurt and A.G. Yodh, "Cerebral hemodynamics in preterm infants during positional intervention measured with diffuse correlation spectroscopy and transcranial Doppler ultrasound," *Opt. Express* **17**(15), 12571–12581 (2009).

51. N. Roche-Labarbe, S. A. Carp, A. Surova, M. Patel, D. A. Boas, R. E. Grant, and M. A. Franceschini, "Noninvasive optical measures of CBV, StO(2), CBF index, and rCMRO(2) in human premature neonates'

brains in the first six weeks of life," *Hum. Brain Mapp* **31**(3), 341–352 (2010).

52. D. A. Boas, L. E. Campbell, and A. G. Yodh, "Scattering and imaging with diffusing temporal field correlations," *Phys. Rev. Lett.* **75**(9), 1855–1858 (1995).

53. D. A. Boas and A. G. Yodh, "Spatially varying dynamical properties of turbid media probed with diffusing temporal light correlation," *J. Opt. Soc. Am. A Opt. Image Sci. Vis.* **14**(1), 192–215 (1997).

54. S. Wray, M. Cope, D. T. Delpy, J. S. Wyatt, and E. O. R. Reynolds, "Characterization of the near-infrared absorption-spectra of cytochrome-Aa3 and hemoglobin for the non-invasive monitoring of cerebral oxygenation," *Biochim. Biophys. Acta* **933**(1), 184–192 (1988).

55. R. Stein, I. Hriljac, J. L. Halperin, S. M. Gustavson, V. Teodorescu, and J. W. Olin, "Limitation of the resting ankle-brachial index in symptomatic patients with peripheral arterial disease," *Vasc. Med.* **11**(1), 29–33 (2006).

56. R. Collins, G. Cranny, J. Burch, R. Aguiar-Ibanez, D. Craig, K. Wright, E. Berry, M. Gough, J. Kleijnen, and M. Westwood, "A systematic review of duplex ultrasound, magnetic resonance angiography and computed tomography angiography for the diagnosis and assessment of symptomatic, lower limb peripheral arterial disease," *Health Technol. Assess.* **11**(20), 1–184 (2007).

57. M. M. McDermott, S. Mehta, K. Liu, J. M. Guralnik, G. J. Martin, M. H. Criqui, and P. Greenland, "Leg symptoms, the ankle-brachial index, and walking ability in patients with peripheral arterial disease," *J. Gen. Intern Med.* **14**(3), 173–181 (1999).

58. R. Fontaine, M. Kim, and R. Kieny, "Surgical treatment of peripheral circulation disorders," *Helv. Chir. Acta* **21**(5–6), 499–533 (1954).

59. A. Kienle and T. Glanzmann, "In vivo determination of the optical properties of muscle with time-resolved reflectance using a layered model," *Phys. Med. Biol.* **44**(11), 2689–2702 (1999).

60. T. J. Farrell, M. S. Patterson, and M. Essenpreis, "Influence of layered tissue architecture on estimates of tissue optical properties obtained from spatially resolved diffuse reflectometry," *Appl. Opt.* **37**(10), 1958–1972 (1998).

61. M. C. P. van Beekvelt, M. S. Borghuis, B. G. M. van Engelen, R. A. Wevers, and W. N. J. M. Colier, "Adipose tissue thickness affects in vivo quantitative near-IR spectroscopy in human skeletal muscle," *Clin. Sci.* **101**(1), 21–28 (2001).

62. A. V. Kurpad, C. Kao, P. Dwarkanath, S. Muthayya, A. Mhaskar, A. Thomas, M. Vaz, and F. Jahoor, "In vivo arginine production and nitric oxide synthesis in pregnant Indian women with normal and low body mass indices," *Eur. J. Clin. Nutr.* **63**(9), 1091–1097 (2009).

63. R. Marks and J. P. Allegrante, "Body mass indices in patients with disabling hip osteoarthritis," *Arthritis Res.* **4**(2), 112–116 (2002).

64. T. Durduran, R. Choe, G. Yu, C. Zhou, J. C. Tchou, B. J. Czerniecki, and A. G. Yodh, "Diffuse optical measurement of blood flow in breast tumors," *Opt. Lett.* **30**(21), 2915–2917 (2005).

65. M. J. Kern, J. A. Moore, F. V. Aguirre, R. G. Bach, E. A. Caracciolo, T. Wolford, A. F. Khoury, C. Mechem, and T. J. Donohue, "Determination of angiographic (TIMI grade) blood flow by intracoronary Doppler flow velocity during acute myocardial infarction," *Circulation* **94**(7), 1545–1552 (1996).

66. F. Vandewerf, "Discrepancies between the effects of coronary reperfusion on survival and left-ventricular function," *Lancet* **1**(8651), 1367–1369 (1989).

67. A. Vogt, R. Vonessen, U. Tebbe, W. Feuerer, K. F. Appel, and K. L. Neuhaus, "Impact of early perfusion status of the infarct-related artery on short-term mortality after thrombolysis for acute myocardial-infarction–retrospective analysis of 4 German multicenter studies," *J. Am. Coll. Cardiol.* **21**(6), 1391–1395 (1993).